3-D open boundary magnetic field analysis using infinite element based on hybrid finite element method

Takayoshi Nakata
Okayama University

N. Takahashi
Okayama University

K. Fujiwara
Okayama University

M. Sakaguchi
Okayama University

3-D OPEN BOUNDARY MAGNETIC FIELD ANALYSIS USING INFINITE ELEMENT BASED ON HYBRID FINITE ELEMENT METHOD

T.Nakata, N.Takahashi, K.Fujiwara and M.Sakaguchi
Department of Electrical Engineering,
Okayama University, Okayama 700, Japan

ABSTRACT

A method for analyzing 3-D open boundary magnetic field problems using infinite elements has been developed. The infinite element proposed here has the advantage that the bandwidth of the coefficient matrix and the number of unknown variables are reduced. Moreover, no experience is necessary in determining decay parameters. The effectiveness of the infinite element is illustrated by comparing the accuracy and the CPU time when various boundary conditions are applied.

1. INTRODUCTION

Various methods of analysis for the open boundary problems have been investigated[1-8]. Although the coupled finite element and boundary element method is popular[7], the method has the disadvantage that the coefficient matrix concerned with the boundary elements becomes dense. If the infinite element based on the hybrid finite element method[9] is used, this difficulty can be avoided.

In this paper, a new formulation of the infinite element for 3-D magnetic field analysis is proposed. This infinite element has the advantage that the bandwidth of the coefficient matrix and the number of unknown variables are less than those of the conventional infinite elements[4,7]. It does not require the evaluation of decay parameters by experience[2]. Moreover, the special technique[3] of numerical integration for calculating the coefficients on infinite elements is not required. In order to demonstrate the effectiveness of the method, an air-core coil is analyzed using the infinite elements.

2. METHOD OF ANALYSIS

In this method, the whole region is divided into the region R_{in} of interest which includes windings, iron cores and magnets and the infinite region R_{ex} as shown in Fig.1. The region R_{in} of interest and the infinite region R_{ex} are discretized by ordinary finite elements and infinite elements respectively. When tetrahedral finite elements are used, the infinite element forms a frustum of a triangular pyramid as shown in Fig.1.

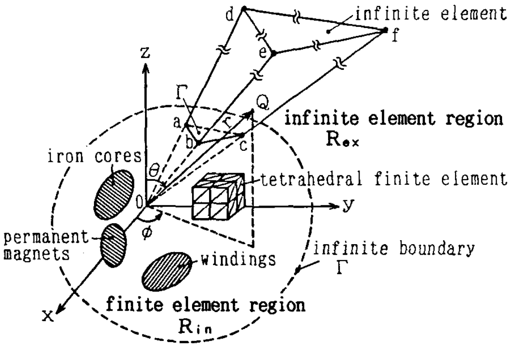

Fig.1 Infinite element.

The functional of the infinite region is represented as follows[9]:

$$\chi_{ex}=\mu\iint_{\Gamma}\tilde{\Omega}\frac{\partial\Omega}{\partial n}d\Gamma-\frac{1}{2}\mu\iint_{\Gamma}\Omega\frac{\partial\Omega}{\partial n}d\Gamma \qquad (1)$$

where Ω is the magnetic scalar potential which is represented as an analytical solution of Laplace's equation governing the infinite region. $\tilde{\Omega}$ is the magnetic scalar potential defined on the surfaces of the infinite element. n denotes the outward normal direction to the surface. μ is the permeability in the infinite region. Γ denotes the boundary between the region of interest and the infinite region as shown in Fig.1.

Ω is represented in the spherical coordinate system as follows[10]:

$$\Omega=\sum_{n=0}^{N}\frac{1}{r^{n+1}}\sum_{m=0}^{n}(\xi_{nm}\cos m\phi+\eta_{nm}\sin m\phi)P_n^m(\cos\theta) \qquad (2)$$

where r is the distance from the origin to the point Q in the infinite element. ϕ and θ are the angles from the x- and z-axes respectively. P_n^m(n=0,---,N, m=0,---,n) denote Legendre polynomials. N denotes the number of terms used to approximate the solution in the infinite region. Although ξ_{nm} and η_{nm} are treated as unknown variables in other methods[4,7], it is not necessary to treat them as unknown variables in the infinite element proposed here, because they can be eliminated by applying the condition for stationarity to the functional of Eq.(1)[9]. The magnetic scalar potential in the infinite region Ω and that on the surface of the infinite element $\tilde{\Omega}$ are defined as follows:

$$\Omega=\{A\}^T\{\beta\} \qquad (3)$$

$$\tilde{\Omega}=\sum N_i\tilde{\Omega}_i=\{N\}^T\{\tilde{\Omega}\} \qquad (4)$$

where $\{A\}$ is obtained from Legendre polynomials and $\{\beta\}$ is the coefficient which corresponds to ξ_{nm} and η_{nm} in Eq.(2). N_i is the interpolation function which can be defined on the surface of the infinite element. By replacing Ω and $\tilde{\Omega}$ in Eq.(1) by Eqs.(3) and (4), the following equation can be obtained:

$$\chi_{ex}=\mu(\{\beta\}^T[G]\{\tilde{\Omega}\}-\frac{1}{2}\{\beta\}^T[H]\{\beta\}) \qquad (5)$$

where [G] and [H] are matrices. By applying the condition for stationarity with respect to $\{\beta\}$, the following equation is obtained:

$$[H]\{\beta\}=[G]\{\tilde{\Omega}\} \qquad (6)$$

From Eq.(6),

$$\{\beta\}=[H]^{-1}[G]\{\tilde{\Omega}\} \qquad (7)$$

As $\{\beta\}$ in Eq.(3) can be represented by $\{\tilde{\Omega}\}$ as shown in Eq.(7), the unknown variables ξ_{nm} and η_{nm} in Eq.(2) can be denoted by $\tilde{\Omega}$. As a result, the number of unknown variables (ξ_{nm} and η_{nm}) is reduced.

3. AN EXAMPLE OF APPLICATION

The air-core coil shown in Fig.2 is analyzed by using the $\mathbb{T}$-Ω method[11]. L is the distance from the origin to the boundary Γ. The number N for the approximation in Eq.(2) is chosen to be zero. Figure 3 shows the finite element subdivisions for L=200 and 1000mm.

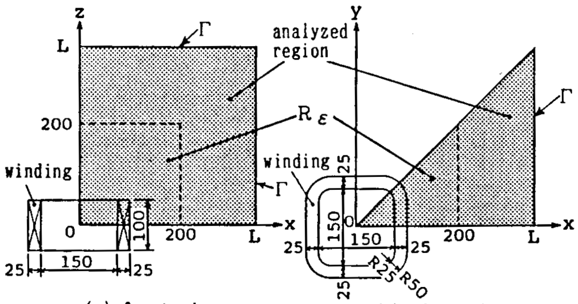

(a) front view (b) plane view
R_ε : region in which error is investigated
Fig.2 Analyzed model.

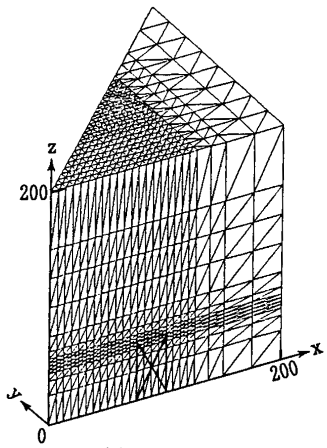

(a) L=200

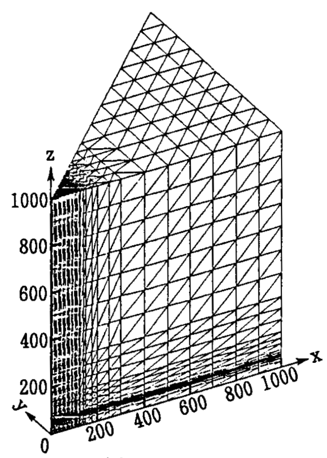

(b) L=1000

Fig.3 Subdivisions for two different values of L.

Figures 4 and 5 show distributions of magnetic scalar potentials for various boundary conditions. Figure 4 shows that the potential distribution for Dirichlet boundary condition becomes similar to that for Neumann boundary condition when L is increased. On the contrary, the potential distribution for the infinite boundary condition is reasonable as shown in Fig.5, even if L is small (=200mm).

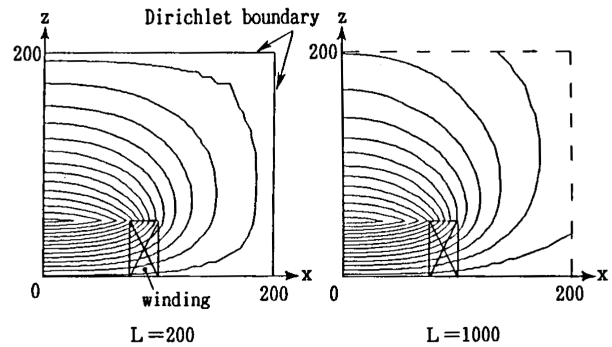

(a) Dirichlet boundary condition

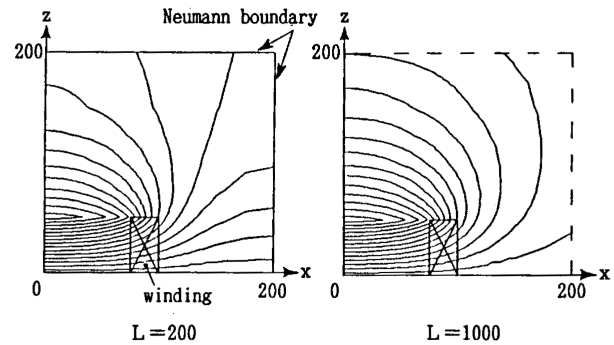

(b) Neumann boundary condition

Fig.4 Distributions of magnetic scalar potentials for Dirichlet and Neumann boundary conditions.

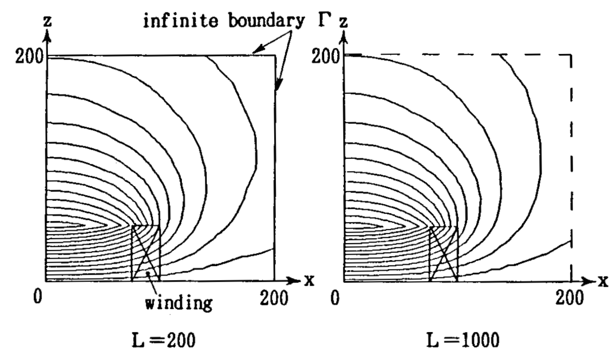

Fig.5 Distributions of magnetic scalar potentials for infinite boundary condition.

Figure 6 shows the effect of the distance L on accuracy and CPU time. The error ε is defined as follows:

$$\varepsilon = \sqrt{\frac{\sum_{e=1}^{N_e}\{B^{(e)}(\mathrm{cal}) - B^{(e)}(\mathrm{true})\}^2}{\sum_{e=1}^{N_e} B^{(e)}(\mathrm{true})^2}} \times 100\ (\%) \qquad (8)$$

where $B^{(e)}(\mathrm{cal})$ is the flux density in the element e which is calculated by the finite element method. $B^{(e)}(\mathrm{true})$ is the flux density when the infinite element is applied at the boundary of L=1000mm. N_e is the number of elements in the region $R\varepsilon$ where the error is investigated as shown in Fig.2. When the distance L is increased, ε for Dirichlet or Neumann boundary approaches that for the infinite boundary asymptotically. ε for the infinite boundary is little affected by L, because the distribution of magnetic scalar potential is reasonable when the infinite element is used as shown in Fig.5, even if L is not so large.

The CPU time T for the infinite boundary at L=200mm is normalized to unity in Fig.6(b). The CPU times for the infinite and Neumann boundaries are nearly the same because of the same number of unknown variables.

Table 1 shows the comparison of the CPU time T* under the condition that the error is the same as that for the infinite boundary at L=200mm. The Table shows

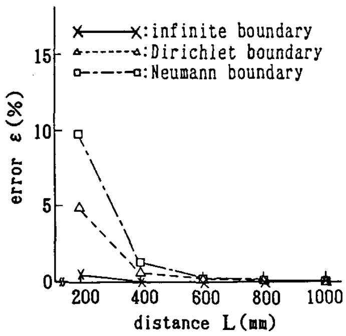

(a) accuracy

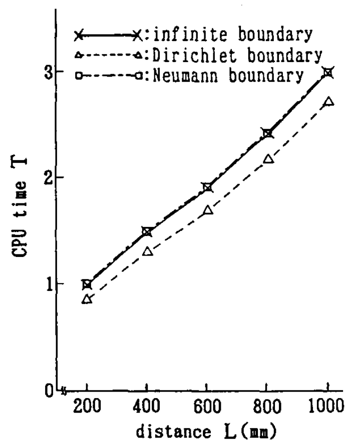

(b) CPU time

Fig.6 Effect of the distance L on accuracy and CPU time.

Table 1 Comparison of CPU time

boundary condition	CPU time T*	distance L (mm)
infinite boundary	1	200
Dirichlet boundary	1.3	400
Neumann boundary	1.9	600

that the CPU time T* for Neumann boundary is 1.9 times as large as that for the infinite boundary, because the analyzed region becomes large (L=600mm) in the analysis using Neumann boundary, in order to obtain the same accuracy as that using the infinite boundary. Therefore, the CPU time for the infinite boundary can be reduced than that for Neumann boundary.

4. CONCLUSIONS

A new infinite element for 3-D open boundary magnetic field analysis has been developed. The computational advantages of the infinite element is shown by comparing the CPU times using the various boundary conditions quantitatively.

The effectiveness of the new infinite element in actual electrical machine problems will be the subject of future investigations.

REFERENCES

[1] C.R.I.Emson : "Methods for the Solution of Open-Boundary Electromagnetic-Field Problems", Proc. IEE, 135, Pt.A, 3, 151 (1988).

[2] P.Bettes : "Infinite Elements", Int. J. Numer. Meth. Eng., 11, 53 (1977).

[3] O.C.Zienkiwicz, K.Bando, P.Bettes, C.Emson and T.C.Chiam : "Mapped Infinite Elements for Exterior Wave Problems", ibid., 21, 1229 (1985).

[4] H.K.Jung, G.S.Lee and S.Y.Hahn : "3-D Magnetic Field Computation Using Finite-Element Approach with Localized Functional", IEEE Trans. Magnetics, MAG-21, 6, 2196 (1985).

[5] J.F.Lee and Z.J.Cendes : "Transfinite Elements : A Highly Efficient Procedure for Modeling Open Field Problems", J. Appl. Phys., 61, 8, 3913 (1987).

[6] M.V.K.Chari, "Electromagnetic Field Computation of Open Boundary Problems by a Semi-Analytic Approach", IEEE Trans. Magnetics, MAG-23, 5, 3566 (1987).

[7] M.V.K.Chari and G.Bedrosian : "Hybrid Harmonic/Finite Element Method for Two-Dimensional Open Boundary Problems", ibid., MAG-23, 5, 3572 (1987).

[8] S.J.Salon and J.D'Angelo : "Applications of the Hybrid Finite Element-Boundary Element Method in Electromagnetics (Invited)", ibid., MAG-24, 1, 80 (1988).

[9] P.Tong and J.N.Rossettos : "Finite-Element Method (Basic Technique and Implementation)" (1977) MIT Press.

[10] P.Moon and D.E.Spencer : "Field Theory for Engineers" (1961) Van Nostrand.

[11] T.Nakata, N.Takahashi, K.Fujiwara and Y.Okada : "Improvements of the T-Ω Method for 3-D Eddy Current Analysis", IEEE Trans. Magnetics, MAG-24, 1, 94 (1988).